Conflict detection in a sequential decision task is associated with increased cortico-subthalamic coherence and prolonged subthalamic oscillatory response in the beta band.

Author List:

Zita Eva Patai[1,2], Tom Foltynie[3], Patricia Limousin[3], Ludvic Zrinzo[3], Rafal Bogacz[2]*, Vladimir Litvak[1]*

[1]Wellcome Centre for Human Neuroimaging, UCL Queen Square Institute of Neurology, London, UK, [2]MRC Brain Network Dynamics Unit, Oxford University, Oxford UK, [3]Functional Neurosurgery Unit, The National Hospital for Neurology and Neurosurgery and Department of Clinical and Movement Neurosciences, UCL Queen Square Institute of Neurology, London, UK

*Equal contribution

Abstract

Making accurate decisions often involves the integration of current as well as past evidence. How the brain achieves this is largely unknown, but the subthalamic nucleus (STN) has been shown to represent immediate conflict in evidence, specifically via theta and beta oscillations. Here we examine the neural correlates of evidence conflict and integration during sequential decision making. Patients implanted with electrodes for deep brain stimulation (DBS) and age-matched healthy controls performed an expanded judgement task, in which they were free to choose how much evidence (cues) to sample before making a decision. Magnetoencephalography (MEG) and STN local field potentials (in patients) were recorded. We found that beta oscillations signalled conflict between cues within a sequence. Specifically, beta power in the STN and cortex first decreased and then increased following cues in the sequence that differed from previous cues. Cortical activity preceded STN activity and premotor cortical-STN coherence was increased in the beta band following the onset of a conflicting cue. Furthermore, the conflict signal in the STN was more persistent over time. These results extend our understanding of cortico-subcortical dynamics of conflict processing, and do so in a context where evidence must be accumulated in discrete steps, much like in real life.

Introduction

Whether it is deciding which method of transportation to take to get to work most efficiently or which horse to bet on to maximize monetary gain, humans are constantly integrating noisy evidence from their environment and past experience, in order to optimize their decisions and to choose the most appropriate action. Often the information comes at intervals, thus necessitating a system that can track incoming signals over time and only commit to making a choice after sufficient evidence has been integrated (Busemeyer & Townsend, 1993; Ratcliff, 1978; Usher & McClelland, 2001). The details of how and where the brain determines if the evidence is sufficient are largely unknown, but it is thought that this process relies on the cortico-basal-ganglia circuit (Bogacz, Wagenmakers, Forstmann, & Nieuwenhuis, 2010). Research in human patients with implanted electrodes for clinical deep-brain stimulation (DBS) treatment has pointed to the role of the subthalamic nucleus (STN) of the basal ganglia as a decision gate-keeper. STN is postulated to set the decision threshold in the face of conflicting information (Frank, 2006). This theory suggests that in situations of conflict between competing responses, the STN activity postpones action initiation until the conflict is resolved. As predicted by the model, STN activity increased for high conflict trials and STN-DBS affected decision making when faced with conflicting evidence (Coulthard et al., 2012; Frank, Samanta, Moustafa, & Sherman, 2007; Green et al., 2013). Furthermore, the decision threshold correlated specifically with changes in STN theta oscillatory power (Cavanagh et al., 2011; Herz, Zavala, Bogacz, & Brown, 2016). The overarching proposal is that oscillatory activity, primarily in the theta and beta bands, in the basal ganglia, reflects immediate inhibition to motor output during situations involving conflict (Frank, 2006), whether it is response, sensory or cognitive uncertainty (Bonnevie & Zaghloul, 2019).

The majority of previous studies in the STN employed paradigms in which the putative processes of conflict detection and setting of decision threshold happened in close temporal proximity. For example, in previously used paradigms such as the flanker task (Zavala et al., 2015), go-no-go (Alegre et al., 2013; Benis et al., 2014), Stroop task (Brittain et al., 2012) and random dot-motion (Herz et al., 2018), evidence was presented simultaneously - as a result such paradigms did not allow to fully disentangle the temporal sequence of the different neural correlates during decision making. To precisely characterize how the neural activity in cortex and the STN changes during the process of evidence accumulation, we used an expanded judgement task (Leimbach et al., 2018), in which evidence was presented at discrete intervals within a trial sequence. This paradigm allowed us to investigate how the neural responses depend on the continual unfolding of evidence extended in time.

An important role in shaping the STN activity is played by the interaction between the cortical circuits and the STN. However, the nature and cortical locus of this interaction has only been examined in a handful of studies. Resting-state coherence between the STN and ipsilateral frontal cortex has shown a peak in the beta band in human patients (Litvak, Jha, et al., 2011; West et al., 2020) as well as rodent models of Parkinson's disease (Magill et al., 2004; West et al., 2018). Additionally, coherence in the theta band from frontal sites (as measured with electroencephalography) to the STN increased during a conflict detection task (Zavala et al., 2014, 2016).

In order to better characterize modulations of STN-cortical connectivity associated with sequential evidence accumulation, we recorded STN local field potential (STN-LFP) simultaneously with whole-head magnetoencephalography (MEG) in Parkinson's disease patients following the implantation of DBS electrodes.

Methods

Participants

We tested 15 patients with a clinical diagnosis of Parkinson's disease (14 male, mean age: 59, range 47-71, two left-handers), following electrode implantation for DBS treatment, before full closure of the scalp, thus allowing for intracranial recordings of the STN (all bilateral recordings, except 1 patient right unilateral and 1 patient with 3 contacts in the left STN and only 2 on the right, this patient was also subsequently diagnosed with Multiple Systems Atrophy). Among tested patients, 11 had Medtronic 3389 electrodes, while 4 had Boston Vercise™ directional leads. The surgical procedures are described in detail in (Foltynie et al., 2011). All patients were assessed on medication (mean Levodopa Equivalent Dosage 1272mg, range: 500-1727.5mg). Unified Parkinson's Disease Rating Scale (UPDRS) part 3 scores were 39.6±14 (mean±standard deviation, range: 18-61) when OFF medication, and 15.4±6.5 (range: 7-30) when ON medication. None of the patients had cognitive impairment (Mini–Mental State Examination (MMSE) scores: mean 28.8, range: 26-30, one patient score missing), clinical depression, or apathy. We recruited 13 age and gender matched controls (12 male, mean age: 57, range 44-70, two left-handers). The patient study was approved by the UK National Research Ethics Service Committee for South Central Oxford and the control study was covered by University College London Ethics Committee approval for minimum risk magnetoencephalography studies of healthy human cognition. The patients did not receive financial compensation and the controls were compensated for their time according to our centre's standard hourly rate.

Task

To investigate the neural basis of evidence accumulation over time, we used the expanded judgement task (Figure 1, similar to a task previously used by Leimbach et al, 2018). Participants were shown a series of images of a mouse facing either left or right. Cues were presented for 200ms, with an inter-stimulus interval of 600ms, so there was 800 ms interval from one onset to another, to which we refer as Stimulus Onset Asynchrony (SOA). Participants were required to judge in which direction the mouse will 'run', based on the probabilities extracted from a series of sequential cue images, and then respond accordingly. The validity of the cues was 70%, such that each cue (left or right mouse) represented the correct choice 70% of the time. The two directions were equally likely across trials, thus chance level in the task was 50%. If the participants responded based on one of the cues only, without accumulating information over time, then their expected success rate would be 70%. Responses were made by pressing a button with the thumb of the congruent hand after a self-chosen number of cues, when the participant felt they had enough evidence to make

a decision. Prior to the recording, the participants underwent a short training session where they were first asked to respond only after seeing a set number of stimuli (between two and ten) and then told that for the main experiment they will decide themselves how many stimuli to observe. This was to ensure that participants made a response decision based on accumulating evidence from a sequence of images rather than just the first stimulus. Participants performed up to 200 trials (Patients: 168±11; Controls: 200 each, except one control who completed 150 trials). Two patients were excluded from the analysis due to poor performance of the task (accuracy at chance level).

Recording and Analysis

Participants performed the task while seated in a whole-head MEG system (CTF-VSM 275-channel scanner, Coquitlam, Canada). For patients, STN-LFP, electrooculography (EOG) and electromyography (EMG) recordings were also obtained using a battery-powered and optically isolated EEG amplifier (BrainAmp MR, Brain Products GmbH, Gilching, Germany). STN-LFP signals were recorded referenced to a common cephalic reference (right mastoid).

All preprocessing was performed in SPM12 (v. 7771, http://www.fil.ion.ucl.ac.uk/spm/, (Litvak, Mattout, et al., 2011)), and spectral analysis and statistical tests were performed in Fieldtrip (http://www.ru.nl/neuroimaging/fieldtrip/,(Oostenveld, Fries, Maris, & Schoffelen, 2011)) using the version included in SPM12.

STN-LFP recordings were converted offline to a bipolar montage between adjacent contacts (three bipolar channels per hemisphere; 01, 12, and 23) to limit the effects of volume conduction from distant sources (for more details see Litvak et al. (2010), Oswal et al (2016)). Four of the patients had segmented DBS leads (Vercise™ DBS directional lead, Boston Scientific, Marlborough, USA). In these cases, we averaged offline the signals from the 3 segments of each ring and treated them as a single ring contact. Thus, for each participant we had a total of 3 STN EEG channels in each hemisphere (except for 2 participants: one with right side electrodes only, thus 3 channels, and one with 1 contact on the right excluded due to extensive noise, thus 5 channels). The LFP data were downsampled to 300Hz and high-pass filtered at 1Hz (Butterworth 5th order, zero phase filter).

A possibly problematic but unavoidable feature of our task was that the stimuli were presented at relatively short SOA not allowing for the power to return to baseline before the next stimulus was presented. Also, the SOA was fixed making entrainment and anticipation possible. These were deliberate design choices to make the task easier for this very difficult patient population prone to attentional difficulties, and to be able to collect a large number of trials for model-based analyses. Any jittering of the SOAs (which would have to go in the direction of increasing their duration) would have led to far fewer trials being collected. The total duration of the recording had to be kept short as the patients were unable to tolerate extended periods of testing. Furthermore, having very long SOA would make it more likely that the participants would resort to explicit counting, which was something we aimed to avoid.

To account for these design issues, we developed an unconventional way of performing time-frequency analysis on these data in the absence of a baseline. We first ran time frequency analysis on continuous LFP data (multitaper method (Thomson, 1982) 400ms sliding window, in steps of 50ms) on *a priori* defined beta power (13-30 Hz average = 21.5Hz; note that when looking at individual participant beta power around the response period, we found a similar band as defined *a priori*: individual mean range: 16.6-28.4Hz; overall min: 11Hz, max: 31Hz). Separately we also estimated the power in the theta band (2-8Hz average = 5Hz, e.g. Herz et al., 2016). The resulting power time series were log-transformed and high-pass filtered at 0.5 Hz (Butterworth 5th order, zero phase filter) to remove fluctuations in power that were slower than our SOA. Afterwards, the power time series were epoched around the presentation of each cue stimulus (-500 to 800ms). We averaged power across contacts within each hemisphere, resulting in 1 left and 1 right STN channel, and we also calculated the mean STN signal by combining hemispheres. For completeness we report individual contact data in the Supplementary Material (Supplementary Figure 1). We used a permutation cluster-based non-parametric test to correct for multiple comparisons across time (the duration of the whole cue epoch (0-800ms) and report effects that survive correction only ($p<0.05$ family-wise error (FWE) corrected at the cluster level).

Similarly to LFP, MEG data were downsampled to 300Hz, and high-pass filtered at 1Hz (Butterworth 5th order, zero phase filter). For sensor-level analysis only, we used the temporal extension of Signal Space Separation method (tSSS), (Taulu & Hari, 2009), to remove the artefacts generated by the presence of ferromagnetic wires (Litvak et al., 2010) from the MEG data. The code we used was an extension to CTF data of the Matlab prototype code for the commercial MaxFilter™ tSSS implementation. The extension was done by the original developer (Samu Taulu) in collaboration with our group and publicly released by MEGIN Oy (Helsinki, Finland). This code is included in SPM12 as 'tSSS toolbox' and its detailed validation on CTF phantom data and comparison to other methods for DBS artefact removal is currently under review (Kandemir et al. in revision, 2020). Using tSSS we also realigned all the head locations to the average location of the control group. For consistency, tSSS preprocessing was applied to both patient and control MEG data.

For the MEG sensor-level time-frequency analysis, we used all channels and a frequency range of 1-45Hz. All other analyses were identical to the LFP pipeline reported above. However, we corrected for multiple comparisons across all MEG channels, timepoints (0-800ms) and frequencies (1-45Hz), and only report effects that survived that correction ($p<0.05$ FWE corrected at the cluster level).

At the source level, the continuous MEG data were projected to source space with Linearly Constrained Maximum Variance (LCMV) beamformer (Veen, Drongelen, Yuchtman, & Suzuki, 1997) using a 10-fold reduced version of the SPM canonical cortical mesh (Mattout, Henson, & Friston, 2007) as the source space (resulting in 818 vertices and the same number of source channels). The source orientation was set in the direction of maximum power. See Litvak et al. (2012) for details on beamforming and Litvak et al. (2010) for details on issues regarding beamformer use for removing artefacts from simultaneous MEG and intracranial recordings. Next, time frequency

analysis was performed on continuous source data the same way as for STN-LFP except the frequencies of interest were informed by the sensor-level analysis. This biased the statistical test for discovery of an effect (cf. double dipping, Kriegeskorte, Simmons, Bellgowan, & Baker, 2009) but our aim in this analysis was post-hoc interrogation of the effects established at the sensor level in terms of their location in the cortex rather than hypothesis testing (Gross et al., 2012). Time-resolved coherence was then computed between the identified cortical sources and STN contacts by going back to raw source time series. The data were epoched (-1000 to 1000ms to increase the window for analysis), and time-frequency analysis was performed as described above with coherence between the sources and the left and right STN also computed from the cross-spectrum. Non-parametric permutation testing between conditions was corrected for multiple comparisons across channels (source vertices), time (0-600ms, note the cue epoch is 0-800ms, however due to the limits of the temporal resolution of the 400ms sliding window, we limited our analysis to the window of uncontaminated data) and frequencies (1-30Hz), and we only report effects that survive correction ($p<0.05$ FWE corrected at the cluster level).

Data availability[1]

The full MEG dataset for controls is available in BIDS format on https://openneuro.org/ and LFP and source data for patients is available on https://data.mrc.ox.ac.uk/. Code and analysis pipeline at https://github.com/zits69/MOUSE_LFPMEG.

Figure 1: Expanded Judgement Task. Participants performed a version of an evidence integration task, with two key elements: 1. the cues were presented sequentially within the trial rather than simultaneously, which allowed us to examine evidence accumulation over time, and 2. The trial duration, i.e. number of cues sampled, was up to the participants, who responded when they felt they had received enough information to make a decision. Participants were required to guess the likely direction (left or right) the mouse 'would run' in. Each cue was 70% valid, i.e. they represented the correct direction 70% of the time if they were to be treated in isolation.

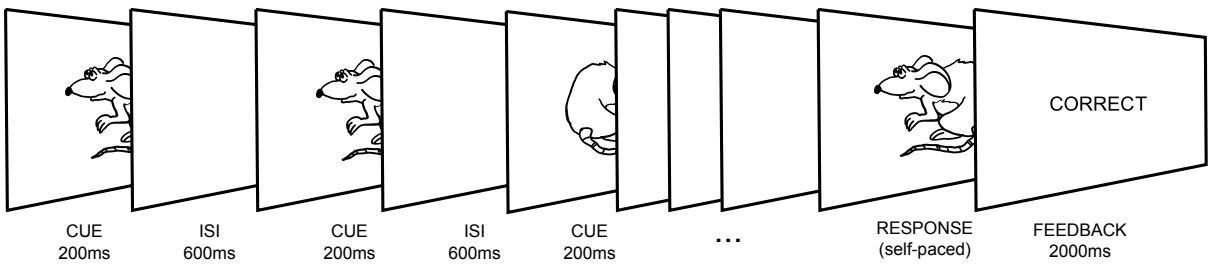

[1] The data will be made available as described here following the acceptance of the paper and full links will be provided.

Results

Patients are able to accumulate evidence over time

Patients waited on average 6.6 stimuli before making a response (6.59±0.52 sem) and their accuracy was significantly above the 70% level expected if they only based their decision on a single cue (80±0.03 sem, t=3.6, p=0.004). Controls waited on average 6.3 stimuli before making a response (6.29±0.46 sem) and were above 70% in their accuracy (88.6±0.01 sem, t=18.4, p<0.001). There was no significant difference between groups in the number of stimuli viewed before making a choice (t=0.42, p-value = 0.68), but patients had lower accuracy (t=-2.99, p=0.0009) and slower reaction time (as measured from the onset of the last cue before a response was made, t=2.16,p=0.041). To explore potential strategies participants could have used in the task, we compared performance in both groups to an agent that would have been an optimal observer, and would choose to respond left if the number of left cues was higher than the number of right cues, to respond right for a larger number of right cues, and would choose randomly if the numbers were equal. In other words, for each participant, we calculated the accuracy they would have achieved had they integrated evidence optimally, but we used the stimuli sampled by the participant on each trial. We found that controls and patients had significantly lower accuracy (controls: p=0.019, patients: p=0.0076) than an ideal observer would have, based on the same cue sampling (89% for controls and 87% for patients). Next, we asked whether participants were just solving the task by responding after they spotted two of the same stimuli in a row (i.e. after the first 'same' pair). We permuted all the possible stimulus sequences that were used in the experiment 100,000 times, calculated the accuracy of an agent that would commit to a choice after the first pair is seen (e.g. left-left), and found the limit to be 80.6%. While patients were not significantly different (p>0.1), controls did perform better than this strategy would suggest (p<0.001). Nevertheless, analyzing behavioural data with explicit mathematical models demonstrated that the patients were not using the strategy of responding after two same cues only, but rather relied on imperfect evidence accumulation. See Supplemental Material for details.

STN beta power shows persistent activity to local conflict during evidence accumulation

In order to investigate how the STN represents the inconsistencies when faced with conflicting evidence, we separated all cues into two categories: 'same' or 'different' to the one immediately before it (we term this 'cue i', Figure 2A). In our analyses of neural responses to cues, we excluded the first cues in a sequence, because it is not possible to classify them as 'same' or 'different', and last cues seen as they overlapped with the response period. Thus, if a participant experienced this sequence of mouse images: 'left-right-left-left-right', the analysed conditions would be 'different-different-same'.

We found that only beta oscillations responded to local conflict, generating a significant difference between 'same' and 'different' cues (cue 'i' in Figure 2B left panel) starting around 100ms after cue onset. Beta also showed a significant difference in the subsequent cue (i+1), with 'different' cues showing an increase in beta power, thus

conflicting information on cue i results in increased beta power on cue i+1 (see Supplementary Figure 2 for details), a pattern of activity that is consistent with response inhibition. These effects were greatly reduced in the theta band, with an effect of condition only briefly detectable during cue ‘i+1’ (Figure 2B-C, right panel).

We correlated across participants the changes in beta power at each cue (cue ‘i’, ‘i+1’, ‘i+2’) with behavioural measures (accuracy, reaction time, the number of stimuli sampled). We found a significant negative relationship ($r=-.5$, $p=0.048$) only between the reaction time and the difference in beta power between ‘different’ and ‘same’ at cue ‘i+1’ (averaged over the significant time window, i.e. 750-1100 ms after onset of cue i). However, this did not survive Bonferroni correction. When correlating trial-wise beta power with reaction time or the number of stimuli sampled at the single participant level, we did not find any significant effects.

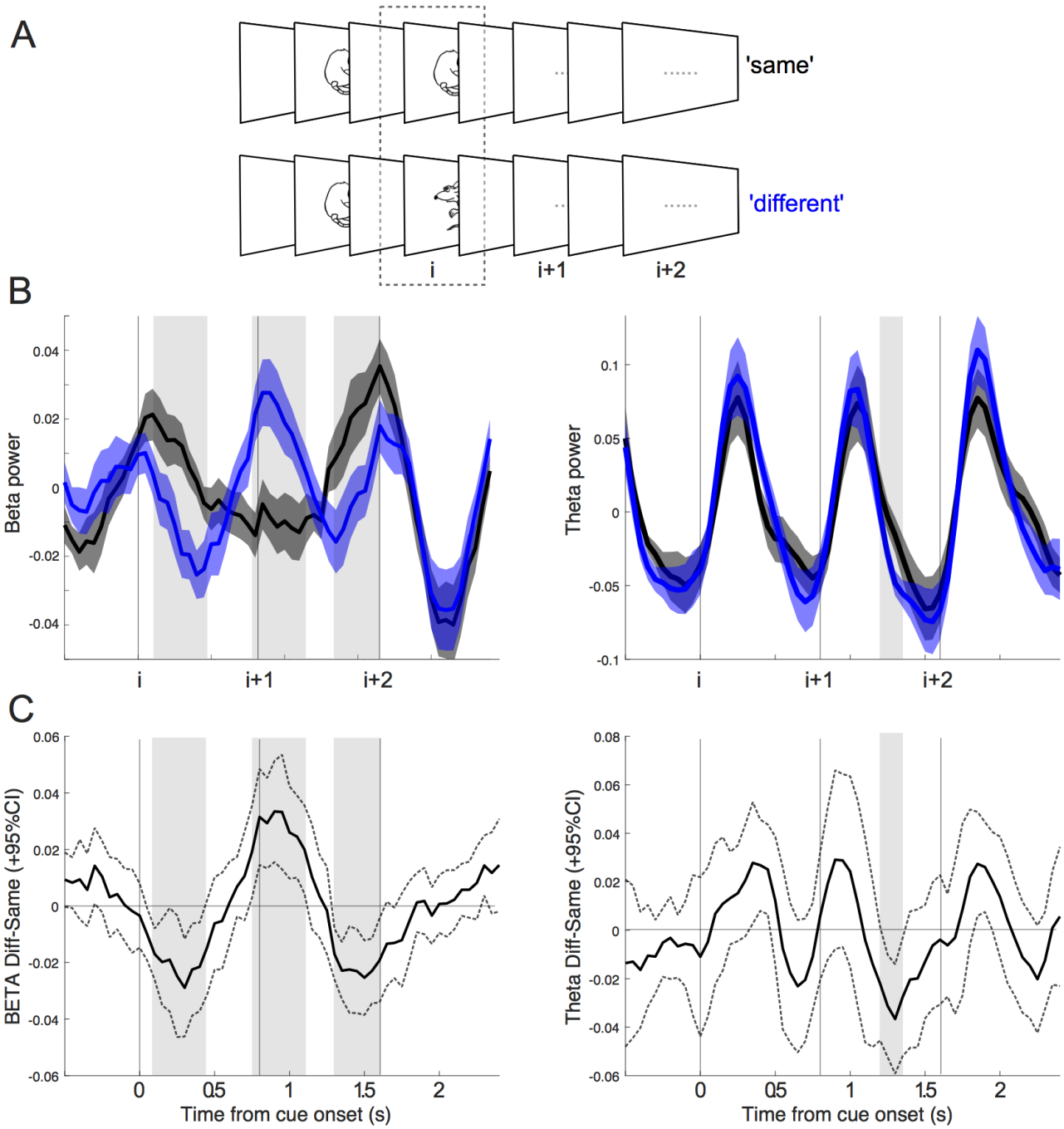

Figure 2: Beta signalled local conflict, and carried over this effect to the next cue in a sequence. A) Notation used in the paper. Let us consider an arbitrary cue i in a sequence, where i>1: If cue i-1 is the same as cue i, then we would call this the 'same' condition, and 'different' otherwise. We also plot the subsequent cues (i+1, i+2) for carry-over effects, but these are collapsed across cue type, left or right (see Supplemental Figure 2 for more detail). B) Left panel: Beta carried information locally as well as over to the next cue, with increased beta power for the 'different' condition. Right panel: Theta only carried mismatch information at the next cue in the sequence. Significant time periods are highlighted with shaded grey bars. Vertical lines show onset of cues in the sequence. The shaded error bars show standard error of the mean. C) Difference waves of conditions ('different' minus 'same') with 95% confidence intervals shown by the dotted lines. After an initial dip there is a clear increase in beta power following the conflicting cue (i) starting just before the onset of

cue i+1. Significant time periods are highlighted with shaded grey bars copied from panel B for comparison. Note that the apparent onset of the effect before zero is due to limited time resolution of the time-frequency decomposition.

Cortical activity reflects rapid but non-persistent conflict detection

We investigated sensor-level MEG signals from controls and patients in response to conflict detection within the sequence. As with the STN, widespread activity over central sensors was found to signal conflict – with an initial dip followed by an increase in beta power on ‘different’ trials (Figure 3). This effect was significant in controls (50-400ms, 11-28 Hz) and when combining the two groups (0-350ms, 11-22Hz) but not in patients alone. This may be due to the non-optimal positioning in the MEG helmet for the patient group, which was dictated by the need to accommodate externalized DBS leads and connectors. Importantly, the time-course of this effect was quicker than the STN (Figure 2B), with conflicting information not persisting until the onset of the next cue in the sequence.

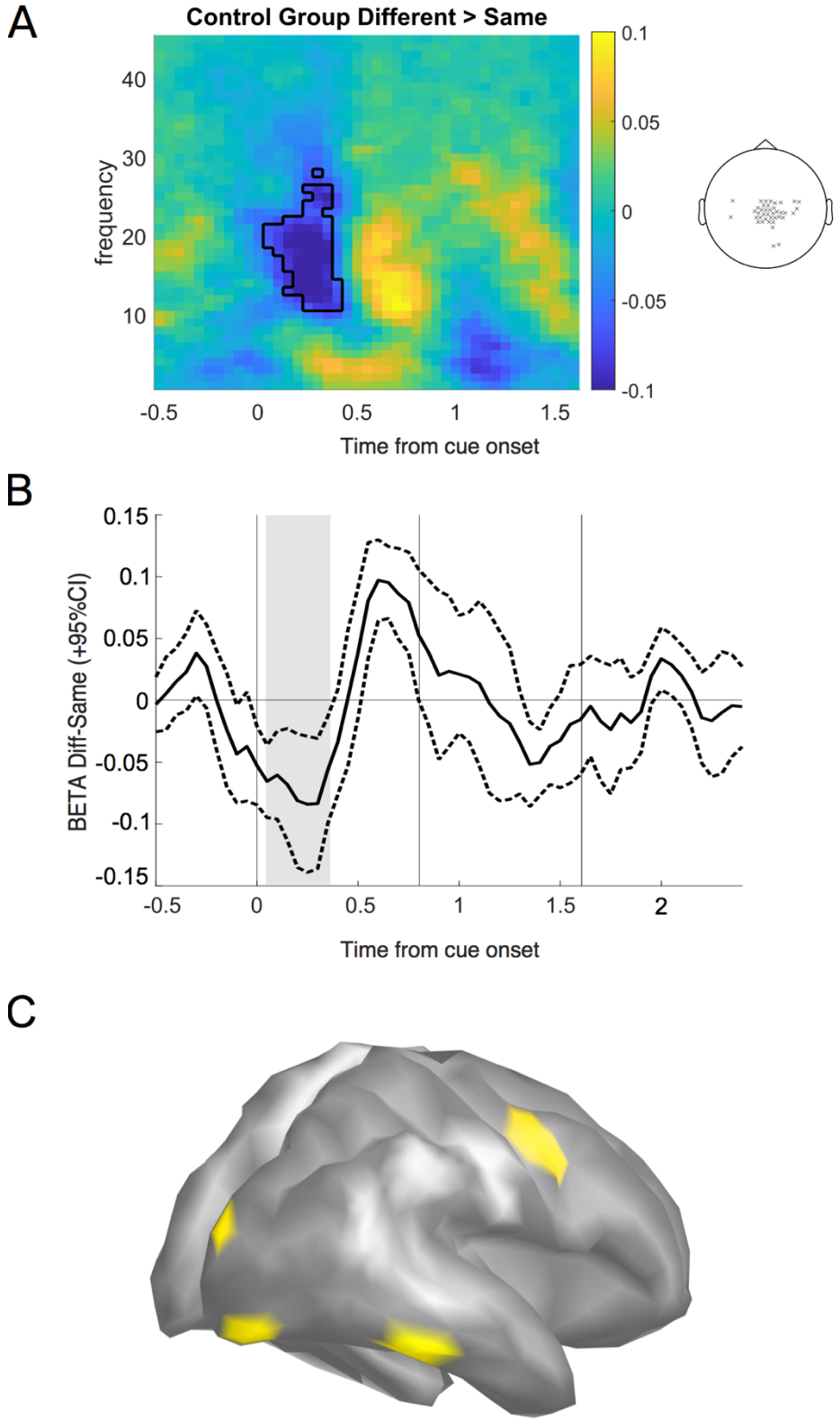

Figure 3: Cortical activity to conflict parallels STN but peaks earlier on average and has a shorter time course. A) Top: Time-frequency plot showing significant times and frequencies when contrasting 'different' vs 'same' cues. Significant channels are shown on the right. B) Difference wave for the beta (13-30Hz) band, as represented in Figure 2B. The dotted lines indicate 95% confidence intervals and the significant time period (the same as in A) is highlighted with shaded grey bars. Note that the apparent onset of the effect before zero is due to limited time resolution of the time-frequency decomposition. C) Source localization placed these effects in three right-lateralized areas: occipital pole, ventral temporal cortex and premotor area BA6.

Coherence is increased between STN and frontal cortex during conflict

We used beamforming in a combined sample of patients and controls to localize the source of the ‘same-different’ effect (averaged over: 200-400ms, 10-31Hz), and found four right-hemisphere lateralized peaks (Figure 3C): occipital pole (2 peaks: MNI 59, -53, -21; 35, -89, -16), ventral temporal cortex (MNI 19, -98, 14) and premotor cortex/BA6 (MNI 52, -7, 44). Next, we measured in patients the coherence between these cortical vertices and both the left and right STN-LFPs, separately. The coherence spectra were averaged over adjacent vertices resulting in 3 cortical sources. We found a significant increase in coherence between the right frontal cortex and the right STN (Figure 4) in the beta band (17-21Hz), shortly after the onset of ‘different’ cues (0-240ms), suggesting that ipsilateral cortical-subthalamic coherence is increased in the face of conflict in the right hemisphere. No other sources, nor the left STN showed any significant effects.

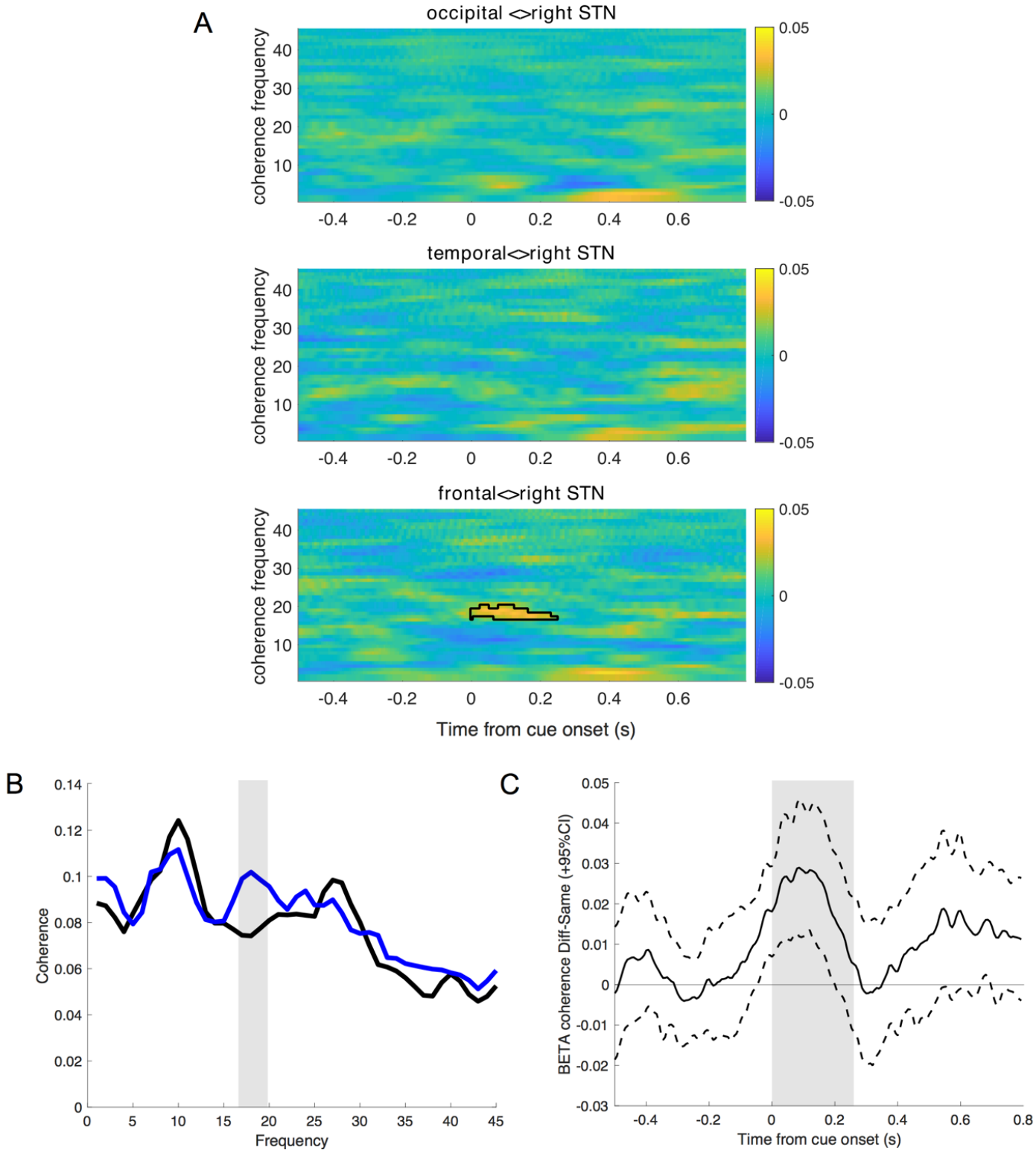

Figure 4: Increased coherence between right frontal cortex and right STN during conflict. A) Plotted are the time-frequency plots of coherence between the right STN and the three cortical sources. Beta coherence is increased for the 'different' condition, for 0-240ms after cue onset. B) Frequency spectra of 'same' (black) and 'different' (blue) trials during the significant time period from A. Grey area highlights significant frequencies: 17-20Hz. C) Time-course of coherence plotted as a difference wave between conditions. The dotted lines indicate 95% confidence intervals and the significant time period is highlighted with shaded grey bars (0-240ms). Note that the apparent onset of the effect before zero is due to limited time resolution of the time-frequency decomposition.

Other variables related to decision making

In addition to conflict, we analyzed whether other variables occurring in theoretical models of decision making were reflected in neural activity. First, we explored if STN represents the normalization term in Bayes theorem as proposed in a computational model (Bogacz & Gurney, 2007). This model suggests that the basal ganglia compute the reward probabilities for selecting different actions according to Bayesian decision theory (Bogacz & Gurney, 2007; Bogacz & Larsen, 2011). These probabilities are updated after each stimulus and the updated information is fed back to the cortex via the thalamus. An action is initiated when the expected reward under a particular action exceeds a certain threshold. The model attributes a very specific function to the STN: ensuring that if the probability of one action goes up, the probabilities of the others go down at the same time by normalising all probabilities so that they add up to one. To fulfil this function, the model predicts that the activity in STN is proportional to a logarithm of the normalization term in Bayes theorem (P(stimulus)). We tested this prediction and did not find any evidence supporting it in our data (Figure 5A; details of methods in Supplemental Methods).

It has been previously reported that the Bayesian normalization term was encoded in the power of beta oscillations in the cortex in a decision task in which the evidence was also presented gradually (Gould, Nobre, Wyart, & Rushworth, 2012). Consequently, we explored whether there was any coding of the Bayesian normalization term in the cortex, by running a regression across all times, frequencies and channels, with cue identity (‘same’ or ‘different’) as a control variable. We found a significant effect in the beta band towards the end of the cue period (Figure 5B), matching in timing and frequency to those reported by Gould et al. (2012).

We also explored whether there was a signal reflecting the magnitude of accumulated evidence in the STN and cortex, but we did not find such a signal (STN: Figure 5A, cortex: not shown). Finally, given previous reports of decreasing beta power as a result of increasing working memory load (Zavala, Jang, & Zaghloul, 2017), we also ran a regression on beta power including the serial position at each cue stimulus, and found no significant effects (see Figure 5A, ‘stimulus number’). Instead as can be seen in Figure 5A, beta power carried information about the similarity of the stimulus to the previous one (‘same’ or ‘different’), but no signal pertaining to of any form of evidence accumulation. There were no significant effects of any of the above regressors on theta power.

A traditional view of the STN places a role on theta power in the process of setting decision thresholds in the face of conflict - in our paradigm we could directly test whether this threshold had a behavioural correlate, namely the number of samples seen before committing to a response. We divided the second cue in a sequence into two conditions again: ‘same’ or ‘different’ as the first cue in the sequence. Behaviourally we found that indeed participants sample more evidence (or make more ‘draws’) after an initial ‘‘different’’ stimulus pair (mean samples after different: 5.07, mean after ‘same’: 4.8, p=0.007). We ran a regression between theta power at the second stimulus (i.e. first possible point of conflict) and the number of stimulus ‘draws’ thereafter, in other words the number of stimuli viewed before a response was made.

If indeed theta sets a threshold for subsequent decision making, then we would predict that theta should scale with the number of upcoming stimuli, which can in turn be viewed as a proxy for the amount of evidence needed to make a decision. We found that theta power after the second cue was related with the number of stimuli subsequently seen before choice, such that lower theta after a ‘same’ cue resulted in more samples drawn, and this was lower than theta power after ‘different’ cues (between 300-400ms after cue onset). However, this effect did not survive cluster correction for multiple comparisons across the cue period. No such relationship was found for beta power.

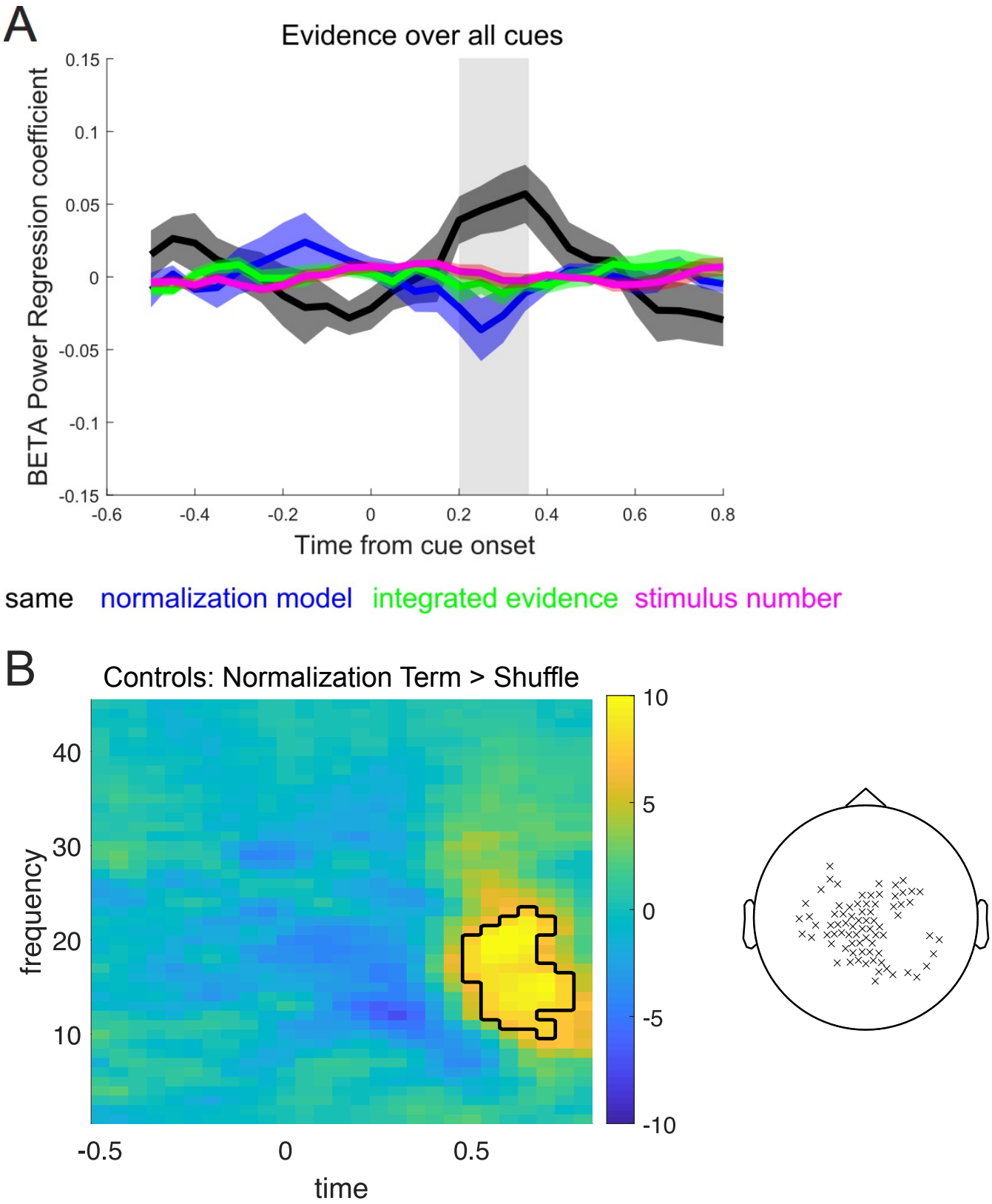

Figure 5: STN activity encodes conflict via beta oscillations, but does not code variables related to accumulation of evidence. A) A linear regression of beta and theta in the STN revealed that the only clear signal was related to the identity of the cue ('same' or 'different', shaded in grey) in beta power only, and there was no encoding of Bayesian normalization, as proposed previously (Bogacz & Gurney, 2007; Bogacz, Martin Moraud, Abdi, Magill, & Baufreton, 2016), nor was there encoding of integrated evidence, or stimulus number in the sequence of cues in a trial. **B)** We found evidence for the Bayesian normalization term in controls at the sensor level reproducing the result of Gould et al. (2012).

Discussion

In this experiment we present novel evidence pertaining to the role of the STN and cortico-subthalamic communication during sequential decision making, using a task in which participants had to integrate evidence over discrete time periods, with no constraints on how many samples they could observe before making a decision. We find evidence for persistent conflict representation in the STN via beta oscillations, and increased coherence with frontal cortex.

Representation of Conflict in the STN

We found that activity in the beta band carried information about conflict over the course of the sequence of cues as evidence unfolded over time. Beta power was initially lower for cues that were 'different' to the one immediately before and continued to increase across the next cue in the sequence. We interpret the increase of beta power as a stop signal, or a break on motor output (Alegre et al., 2013) inhibiting a response after an inconsistent cue. It has been shown before that activity in the beta band carries conflict information across trials (Zavala et al., 2018), but we also show this effect within a trial, as conflict arises within the sequence of evidence. Beta power increases have also been reported when a 'surprise' stimulus is presented (Wessel et al., 2016), and STN activity measured with fMRI has been shown to increase when conflict is detected or arises due to too much choice (Keuken et al., 2015) – though this has been shown on singular events rather than over the course of evidence accumulation. Moreover, the majority of trials ended on a 'same' cue (Supplementary Table 1), which is in line with an overall increase in beta synchronization after 'different' cues and lower probability of responding. As for the initial decrease in beta power, this has been reported before as a slower 'resynchronization' of beta during incongruent cues (Brittain et al., 2012), and also as a pathological signal inhibiting the integration of melodic sequences (Ruiz et al., 2014).

Interaction between STN and Cortex

Interestingly, the overall picture was very similar in cortex, with two main differences: the 'same'-'different' effect on average peaked earlier in the cortex (Figure 6), and also did not carry over to the next cue in the sequence (Figure 3A). A possible interpretation is that the cortex signalled the immediate conflict to STN, which then maintained a more persistent activity to inhibit responses (Brittain et al., 2012; Fife et al., 2017). When we localized the sources of the 'same'-'different' effect, we found three right-lateralized areas in the cortex which showed a conflict signal: occipital, temporal and frontal cortex. Only the frontal source, located in premotor cortex/supplementary motor area (BA6) showed a significant coherence with the ipsilateral STN only, namely an increase in beta coherence at the onset of a 'different', or conflict, cue (Figure 4). Critically, this is in contrast to the overall *decrease* in beta power during most of this time period, both in the STN and the cortex (Figure 6) ruling out 'power confound' as a possible explanation (Muthukumaraswamy & Singh, 2011). Due to the fact that this is only a relatively weak effect with a short time course, we were unable to reliably estimate the directionality of coherence, but previous reports on resting-state data have shown

cortex to drive STN activity (Litvak, Jha, et al., 2011), which is in line with the finding here that the ‘same’-‘different’ effect seems to peak earlier in the cortical signal.

The right BA6 is well-established as a cortical region involved in response-inhibition/initiation and cognitive control (Aron, 2011; Buch, Mars, Boorman, & Rushworth, 2010; Chambers et al., 2007; Simmonds, Pekar, & Mostofsky, 2008). Other areas did not show any significant coherence effects, although superior temporal gyrus is coupled to the STN in the alpha band during rest (Litvak, Jha, et al., 2011) and during simple motor output (Hirschmann et al., 2013) and coupling strength is modulated by discrete movements (Oswal, Brown, & Litvak, 2013) suggesting that this circuit could be involved in motor planning.

While it is well-established that the cortex communicates with the STN via two anatomically defined pathways, the indirect and the hyperdirect pathways (Albin, Young, & Penney, 1989; DeLong, 1990; Nambu, Tokuno, & Takada, 2002), recent evidence suggests the existence of two separate coherent beta oscillatory networks between the cortex and the STN (Oswal, Beudel, et al., 2016) with the low beta network (13-21Hz) likely corresponding to the indirect pathway from lateral prefrontal regions to the STN via the striatum and external Globus Pallidus. Here we find evidence for a similar pattern of oscillatory connectivity, which may have implications for understanding the involvement of various pathways in sequential evidence accumulation.

Brief cortical beta responses triggering a prolonged STN are in agreement with the suggestion that the cortex initiates abnormal subcortical beta activity that is then amplified by the subthalamo-pallidal circuit (Pavlides, Hogan, & Bogacz, 2015). Although, here our information about STN activity and cortico-subthalamic coherence comes from Parkinson’s patients, one hypothesis that could be considered is that our experiment revealed an aspect of the healthy functioning of this circuit that is then hijacked by the disease resulting in the generation of abnormal STN activity that impairs movement. This interpretation is supported by the fact that our patients performed the task on dopaminergic medication when their pathological STN beta is known to be reduced (Mallet et al., 2008) and the functioning of the cortico-basal ganglia circuit is closer to the healthy state.

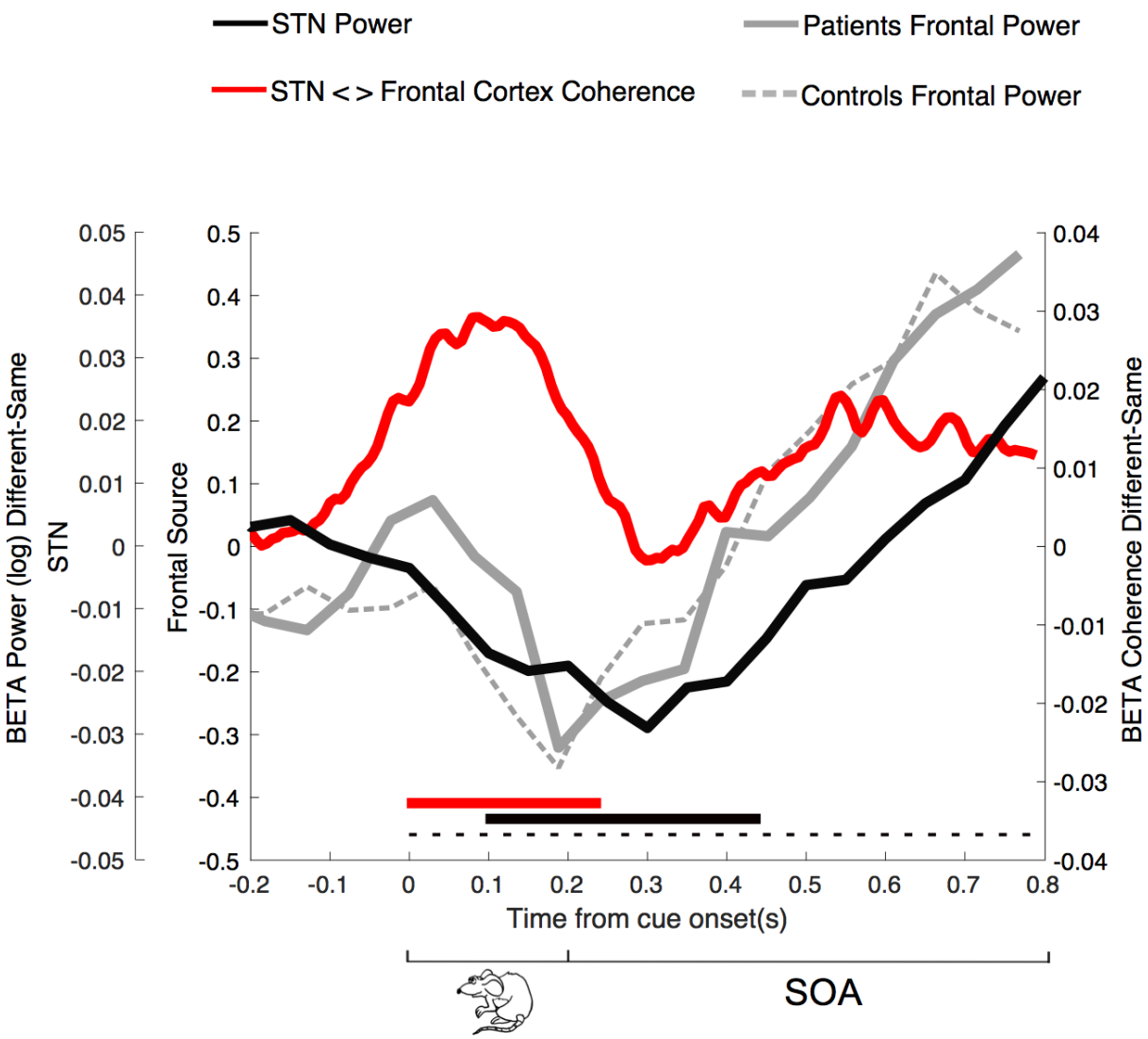

Figure 6: Time-course of beta power and coherence differences between conditions. This figure shows a summary of findings presented in Figure 2C and 4C as well as source power time courses to facilitate the comparison of timings of the effects. While the STN LFPs, sensor-level MEG signal (not shown) and the beamformed frontal source in patients and controls all show a decrease in beta power immediately after 'different' cues (onset at zero seconds), the beta coherence between the STN and frontal cortex (red line) shows a concurrent increase. Of note is that the cue was on screen for 200ms (out of total SOA of 800ms), which is the time window similar to that in which significant coherence increase was found. Coloured lines at the bottom of the plot indicate the times of significant differences between 'same' and 'different' cues for each measure plotted, red: right STN- right frontal coherence, black: STN power, dotted: MEG sensor level power (time course not shown). The frontal source was not submitted to separate statistical testing as it is derived from the MEG sensor data. Note that the apparent onset of effects before zero is due to limited time resolution of the time-frequency decomposition.

Where is the theta conflict signal?

The predominant theory of STN function, and also that of the cortex during conflict detection, is the involvement of theta oscillations (Cavanagh & Frank, 2014). A large portion of empirical findings on the STN shows that it carries conflict information via the theta band (Cavanagh et al., 2011; Herz et al., 2016; Zavala et al., 2015, 2016, 2018, 2017). Yet in our task we only found a weak effect of theta modulation, in the cue following a conflict (cue i+1). This effect was present only in the STN, and no theta effects were found in the cortex. Moreover, this manifested as reduced theta synchronization to 'different' cues, which is the opposite of the standard reported theta increase during conflict. One explanation may be the task design, as it differs from previous paradigms: there are no long intervals over which to examine slow oscillations, such as theta. Our results, therefore, though focussed on theta power (2-8Hz), may be dominated by evoked potentials, as cues were presented in a fixed, relatively short duration (200ms, with 600ms inter stimulus interval) sequence. Additionally, here conflict is defined over the course of multiple cues, not on a singular trial in isolation. Thus, the integration of conflict over time may in fact be driven by different signals – beta may represent a more consistent inhibition during conflicting incoming information. Nevertheless, others have also reported a lack of theta effects in the STN during a stop-signal task (Bastin et al., 2014).

In terms of STN connectivity, two previous reports have found increased theta coherence during conflict with medial frontal cortex (Zavala et al., 2014, 2016). We found increased coherence in the beta band, and a more lateral frontal area. The other reports, however, used EEG rather than MEG. This might be critical in our case as MEG is known to be less sensitive to the anterior cingulate theta conflict signal that most of the authors consider to be the source driving theta responses in the STN. This could be due to higher variability of the MEG theta conflict signature topographies that do not survive averaging across subjects and require a different kind of analysis approaches (Zuure, Hinkley, Tiesinga, Nagarajan, & Cohen, 2020). Additionally, neither of these reports investigated changes in beta coherence, and thus it is unclear whether these effects existed at all. Finally, the previous reports analysed coherence during a cue period that was uninterrupted by additional incoming stimuli (as is the case in our task), and thus low frequency oscillations may be clearer in those studies, as discussed above.

Given the constraints of the paradigm, we were unable to test how pre-trial baseline activity may have affected subsequent cue processing, for example if intrinsic low frequency power predicted the number of cues to be sampled in the upcoming trial. More detailed investigations are needed to confirm the effect of ongoing fluctuations in attention and responses to continuous feedback in how decision thresholds are set over the course of multiple trials.

Updating models of the STN

The role of the STN in decision making has been formalized in several computational models that account for a range of findings related to anatomy and physiology of the cortico-basal ganglia circuit including the STN. An influential model proposed by Frank

(2006) suggests that in situations of conflict between competing responses an increased activity of STN postpones action initiation (Frank, 2006). This model proposes that STN is essential for decision making since it ensures that an action is only selected when it has high evidence, relative to the other options. Another model proposed by Bogacz & Gurney (2007) suggests that the basal ganglia compute the reward probabilities for selecting different actions according to Bayesian decision theory (Bogacz & Gurney, 2007; Bogacz & Larsen, 2011). According to that model, STN computes the normalization term in Bayes theorem, which ensures that the updated probabilities add up to 1 across the actions. While in our task we did not find conclusive evidence that the STN is encoding Bayesian normalization (Figure 5A), we observed its participation in conflict processing, yet not in the predicted theta frequency band (see previous section). It is important to remember that, despite being on medication, these experiments were performed in patients whose neural circuitry has been affected by advanced Parkinson's disease. Control participants did show activity encoding Bayesian normalization at the cortical level (Figure 5B), in agreement with a previous study (Gould et al., 2012). In fact, the timing and frequency of this activity was remarkably similar to that found by Gould et al. in a more complex paradigm (cf. their Figure 8). Thus, one cannot rule out the possibility that the Bayesian normalization is encoded by the STN of healthy individuals, but testing this hypothesis would require a different experimental technique (e.g. recording of STN neural activity from animals during an analogous decision making task, such as a task employed by Brunton, Botvinick, & Brody, 2013). An alternative explanation is that the Bayesian normalization term is computed not in the STN but elsewhere. However, this computation requires a highly specialized circuit and it is unclear where else such circuit could be located in the brain

We did not find encoding of pure evidence integration or response certainty, as in previous reports (De Lange, Jensen, & Dehaene, 2010; Gould et al., 2012; Gould, Rushworth, & Nobre, 2011). Furthermore, our behavioural modelling revealed that both patients and controls were using an imperfect form of evidence integration to make their responses. Given that we were unable to measure ongoing eye-movements during task performance – which would have provided a clearer picture of attention to the individual cues – it is hard to tease apart which individual cues *actually* contributed to the decision.

Conclusion

Contrary to the emphasis on theta signals in the context of immediate conflict, here we find a prominent role for beta oscillations in signalling conflict across the whole of a sequence of evidence. We find that both cortex and the STN carry this signal, with cortex peaking on average earlier, and find that coherence is increased between these areas when conflict is detected. We showed that a brief cortical response to conflict in the cortex triggers a more prolonged response in the STN, which could be an aspect of the healthy function opening the door to pathological amplification of STN beta in Parkinson's.

Acknowledgements

This work has been supported by MRC grants MC_UU_12024/5, MC_UU_00003/1 and BBSRC grant BB/S006338/1. The Wellcome Centre for Human Neuroimaging is supported by core funding from the Wellcome (203147/Z/16/Z). UK MEG community is supported by UK MEG Partnership award from the Medical Research Council (MR/K005464/1). We thank Dr. Ashwini Oswal, Dr. Simon Little, Dr. David Pedrosa, Dr. Damian Herz and Dr. Viswas Dayal for clinical support of patient recordings. We are also grateful to Dr. Tim West, Dr. Hayriye Cagnan and Dr. Simon Farmer for commenting on the manuscript.

Competing interests None.

REFERENCES

Albin, R. L., Young, A. B., & Penney, J. B. (1989). The functional anatomy of basal ganglia disorders. *Trends in Neurosciences*, *12*(10), 366–375.

Alegre, M., Lopez-Azcarate, J., Obeso, I., Wilkinson, L., Rodriguez-Oroz, M. C., Valencia, M., … Obeso, J. A. (2013). The subthalamic nucleus is involved in successful inhibition in the stop-signal task: A local field potential study in Parkinson's disease. *Experimental Neurology*, *239*(1), 1–12.

Aron, A. R. (2011). From reactive to proactive and selective control: Developing a richer model for stopping inappropriate responses. *Biological Psychiatry*, *69*(12), e55–e68.

Bastin, J., Polosan, M., Benis, D., Goetz, L., Bhattacharjee, M., Piallat, B., … David, O. (2014). Inhibitory control and error monitoring by human subthalamic neurons. *Translational Psychiatry*, *4*(9), 2–9.

Benis, D., David, O., Lachaux, J. P., Seigneuret, E., Krack, P., Fraix, V., … Bastin, J. (2014). Subthalamic nucleus activity dissociates proactive and reactive inhibition in patients with Parkinson's disease. *NeuroImage*, *91*, 273–281.

Bogacz, R., & Gurney, K. (2007). The basal ganglia and cortex implement optimal decision. *Neural Computation*, *19*(2), 442–477.

Bogacz, R., & Larsen, T. (2011). Integration of reinforcement learning and optimal decision-making theories of the basal ganglia. *Neural Computation*, *23*(4), 817–851.

Bogacz, R., Martin Moraud, E., Abdi, A., Magill, P. J., & Baufreton, J. (2016). Properties of Neurons in External Globus Pallidus Can Support Optimal Action Selection. *PLoS Computational Biology*, *12*(7), 1–28.

Bogacz, R., Wagenmakers, E.-J., Forstmann, B. U., & Nieuwenhuis, S. (2010). The neural basis of the speed-accuracy tradeoff. *Trends in Neurosciences*, *33*(1), 10–6.

Bonnevie, T., & Zaghloul, K. A. (2019). The Subthalamic Nucleus: Unravelling New

Roles and Mechanisms in the Control of Action. *Neuroscientist*, *25*(1), 48–64.

Brittain, J.-S., Watkins, K. E., Joundi, R. A., Ray, N. J., Holland, P., Green, A. L., … Jenkinson, N. (2012). A role for the subthalamic nucleus in response inhibition during conflict. *Journal of Neuroscience*, *32*(39), 13396–13401.

Brunton, B. W., Botvinick, M. M., & Brody, C. D. (2013). Rats and Humans Can Optimally Accumulate Evidence for Decision-Making. *Science*, *340*(April), 95–99.

Buch, E. R., Mars, R. B., Boorman, E. D., & Rushworth, M. F. S. (2010). A network centered on ventral premotor cortex exerts both facilitatory and inhibitory control over primary motor cortex during action reprogramming. *Journal of Neuroscience*, *30*(4), 1395–1401.

Busemeyer, J. R., & Townsend, J. T. (1993). Decision field theory: A dynamic-cognitive approach to decision making in an uncertain environment. *Psychological Review*, *100*(3), 432–459.

Cavanagh, J. F., & Frank, M. J. (2014). Frontal theta as a mechanism for cognitive control. *Trends in Cognitive Sciences*, *18*(8), 414–421.

Cavanagh, J. F., Wiecki, T. V., Cohen, M. X., Figueroa, C. M., Samanta, J., Sherman, S. J., & Frank, M. J. (2011). Subthalamic nucleus stimulation reverses mediofrontal influence over decision threshold. *Nature Neuroscience*, *14*(11), 1462–1467.

Chambers, C. D., Bellgrove, M. A., Gould, I. C., English, T., Garavan, H., McNaught, E., … Mattingley, J. B. (2007). Dissociable mechanisms of cognitive control in prefrontal and premotor cortex. *Journal of Neurophysiology*, *98*(6), 3638–3647.

Coulthard, E. J., Bogacz, R., Javed, S., Mooney, L. K., Murphy, G., Keeley, S., & Whone, A. L. (2012). Distinct roles of dopamine and subthalamic nucleus in learning and probabilistic decision making. *Brain : A Journal of Neurology*, *135*(Pt 12), 3721–34.

De Lange, F. P., Jensen, O., & Dehaene, S. (2010). Accumulation of evidence during sequential decision making: The importance of top-down factors. *Journal of Neuroscience*, *30*(2), 731–738.

DeLong, M. R. (1990). Primate models of movement disorders of basal ganglia origin. *Trends in Neurosciences*, *13*(7), 281–285.

Fife, K. H., Gutierrez-Reed, N. A., Zell, V., Bailly, J., Lewis, C. M., Aron, A. R., & Hnasko, T. S. (2017). Causal role for the subthalamic nucleus in interrupting behavior. *ELife*, *6*, 1–13.

Foltynie, T., Zrinzo, L., Martinez-Torres, I., Tripoliti, E., Petersen, E., Holl, E., … Limousin, P. (2011). MRI-guided STN DBS in Parkinson's disease without microelectrode recording: Efficacy and safety. *Journal of Neurology, Neurosurgery and Psychiatry*, *82*(4), 358–363.

Frank, M. J. (2006). Hold your horses: A dynamic computational role for the subthalamic nucleus in decision making. *Neural Networks*, *19*(8), 1120–1136.

Frank, M. J., Samanta, J., Moustafa, A. A., & Sherman, S. J. (2007). Hold your

horses: Impulsivity, deep brain stimulation, and medication in Parkinsonism. *Science*, *318*(5854), 1309–1312.

Gould, I. C., Nobre, A. C., Wyart, V., & Rushworth, M. F. S. (2012). Effects of decision variables and intraparietal stimulation on sensorimotor oscillatory activity in the human brain. *Journal of Neuroscience*, *32*(40), 13805–13818.

Gould, I. C., Rushworth, M. F., & Nobre, A. C. (2011). Indexing the graded allocation of visuospatial attention using anticipatory alpha oscillations. *Journal of Neurophysiology*, *105*(3), 1318–26.

Green, N., Bogacz, R., Huebl, J., Beyer, A. K., Kühn, A. A., & Heekeren, H. R. (2013). Reduction of influence of task difficulty on perceptual decision making by stn deep brain stimulation. *Current Biology*, *23*(17), 1681–1684.

Gross, J., Baillet, S., Barnes, G. R., Henson, R. N., Hillebrand, A., Jensen, O., … Schoffelen, J.-M. (2012). Good practice for conducting and reporting MEG research. *NeuroImage*, *65C*, 349–363.

Herz, D. M., Little, S., Pedrosa, D. J., Tinkhauser, G., Cheeran, B., Foltynie, T., … Brown, P. (2018). Mechanisms Underlying Decision-Making as Revealed by Deep-Brain Stimulation in Patients with Parkinson's Disease. *Current Biology*, *28*(8), 1169-1178.e6.

Herz, D. M., Zavala, B., Bogacz, R., & Brown, P. (2016). Neural Correlates of Decision Thresholds in the Human Subthalamic Nucleus. *Current Biology*, *26*(7), 916–920.

Hirschmann, J., Özkurt, T. E., Butz, M., Homburger, M., Elben, S., Hartmann, C. J., … Schnitzler, A. (2013). Differential modulation of STN-cortical and cortico-muscular coherence by movement and levodopa in Parkinson's disease. *NeuroImage*, *68*, 203–213.

Jahanshahi, M. (2013). Effects of deep brain stimulation of the subthalamic nucleus on inhibitory and executive control over prepotent responses in Parkinson's disease. *Frontiers in Systems Neuroscience*, *7*(December), 118.

Keuken, M. C., Van Maanen, L., Bogacz, R., Schäfer, A., Neumann, J., Turner, R., & Forstmann, B. U. (2015). The subthalamic nucleus during decision-making with multiple alternatives. *Human Brain Mapping*, *36*(10), 4041–4052.

Kriegeskorte, N., Simmons, W. K., Bellgowan, P. S., & Baker, C. I. (2009). Circular analysis in systems neuroscience: The dangers of double dipping. *Nature Neuroscience*, *12*(5), 535–540.

Leimbach, F., Georgiev, D., Litvak, V., Antoniades, C., Limousin, P., Jahanshahi, M., & Bogacz, R. (2018). Deep brain stimulation of the subthalamic nucleus does not affect the decrease of decision threshold during the choice process when there is no conflict, time pressure, or reward. *Journal of Cognitive Neuroscience*, *30*(6), 876–884.

Litvak, V., Eusebio, A., Jha, A., Oostenveld, R., Barnes, G. R., Penny, W. D., … Brown, P. (2010). Optimized beamforming for simultaneous MEG and intracranial local field potential recordings in deep brain stimulation patients. *NeuroImage*, *50*(4), 1578–1588.

Litvak, V., Jha, A., Eusebio, A., Oostenveld, R., Foltynie, T., Limousin, P., … Brown, P. (2011). Resting oscillatory cortico-subthalamic connectivity in patients with Parkinson's disease. *Brain*, *134*(2), 359–374.

Litvak, V., Mattout, J., Kiebel, S., Phillips, C., Henson, R., Kilner, J., … Friston, K. (2011). EEG and MEG Data Analysis in SPM8. *Computational Intelligence and Neuroscience*, *2011*, 852961.

Magill, P. J., Sharott, A., Bolam, J. P., & Brown, P. (2004). Brain state-dependency of coherent oscillatory activity in the cerebral cortex and basal ganglia of the rat. *Journal of Neurophysiology*, *92*(4), 2122–2136.

Mallet, N., Pogosyan, A., Sharott, A., Csicsvari, J., Bolam, J. P., Brown, P., & Magill, P. J. (2008). Disrupted dopamine transmission and the emergence of exaggerated beta oscillations in subthalamic nucleus and cerebral cortex. *Journal of Neuroscience*, *28*(18), 4795–4806.

Mattout, J., Henson, R. N., & Friston, K. J. (2007). Canonical Source Reconstruction for MEG. *Computational Intelligence and Neuroscience*, *2007*, 67613.

Muthukumaraswamy, S. D., & Singh, K. D. (2011). A cautionary note on the interpretation of phase-locking estimates with concurrent changes in power. *Clinical Neurophysiology*, *122*(11), 2324–2325.

Nambu, A., Tokuno, H., & Takada, M. (2002). Functional significance of the cortico-subthalamo-pallidal "hyperdirect" pathway. *Neuroscience Research*, *43*(2), 111–117.

Oostenveld, R., Fries, P., Maris, E., & Schoffelen, J.-M. (2011). FieldTrip: Open source software for advanced analysis of MEG, EEG, and invasive electrophysiological data. *Computational Intelligence and Neuroscience*, *2011*, 156869.

Oswal, A., Beudel, M., Zrinzo, L., Limousin, P., Hariz, M., Foltynie, T., … Brown, P. (2016). Deep brain stimulation modulates synchrony within spatially and spectrally distinct resting state networks in Parkinson's disease. *Brain*, *139*(5), 1482–1496.

Oswal, A., Brown, P., & Litvak, V. (2013). Movement related dynamics of subthalmo-cortical alpha connectivity in Parkinson's disease. *NeuroImage*, *70*, 132–142.

Oswal, A., Jha, A., Neal, S., Reid, A., Bradbury, D., Aston, P., … Litvak, V. (2016). Analysis of simultaneous MEG and intracranial LFP recordings during Deep Brain Stimulation: A protocol and experimental validation. *Journal of Neuroscience Methods*, *261*, 29–46.

Pavlides, A., Hogan, S. J., & Bogacz, R. (2015). Computational Models Describing Possible Mechanisms for Generation of Excessive Beta Oscillations in Parkinson's Disease. *PLoS Computational Biology*, *11*(12), 1–29.

Ratcliff, R. (1978). A theory of memory retrieval. *Psychological Review*, *85*(2), 59–108.

Ray, N. J., Brittain, J.-S., Holland, P., Joundi, R. A., Stein, J. F., Aziz, T. Z., & Jenkinson, N. (2012). The role of the subthalamic nucleus in response inhibition: Evidence from local field potential recordings in the human subthalamic nucleus.

NeuroImage, *60*(1), 271–278.

Ruiz, M. H., Rusconi, M., Brücke, C., Haynes, J. D., Schönecker, T., & Kühn, A. A. (2014). Encoding of sequence boundaries in the subthalamic nucleus of patients with Parkinson's disease. *Brain*, *137*(10), 2715–2730.

Simmonds, D. J., Pekar, J. J., & Mostofsky, S. H. (2008). Meta-analysis of Go/No-go tasks demonstrating that fMRI activation associated with response inhibition is task-dependent. *Neuropsychologia*, *46*(1), 224–232.

Taulu, S., & Hari, R. (2009). Removal of magnetoencephalographic artifacts with temporal signal-space separation: demonstration with single-trial auditory-evoked responses. *Human Brain Mapping*, *30*(5), 1524–1534.

Thomson, D. J. (1982). Spectrum estimation and harmonic analysis. *Proceedings of the IEEE*, *70*(9), 1055–1096.

Usher, M., & McClelland, J. L. (2001). The time course of perceptual choice: The leaky, competing accumulator model. *Psychological Review*, *108*(3), 550–592.

Veen, B. D. Van, Drongelen, W. Van, Yuchtman, M., & Suzuki, A. (1997). Localization of brain electrical activity via linearly constrained minimum variance spatial filtering. *IEEE Transactions on Biomedical Engineering*, *44*(9), 867–880.

Wessel, J. R., Jenkinson, N., Brittain, J.-S., Voets, S. H. E. M., Aziz, T. Z., & Aron, A. R. (2016). Surprise disrupts cognition via a fronto-basal ganglia suppressive mechanism. *Nature Communications*, *7*.

West, T. O., Berthouze, L., Halliday, D. M., Litvak, V., Sharott, A., Magill, P. J., & Farmer, S. F. (2018). Propagation of beta/gamma rhythms in the cortico-basal ganglia circuits of the parkinsonian rat. *Journal of Neurophysiology*, *119*(5), 1608–1628.

West, T. O., Farmer, S. F., Magill, P. J., Sharott, A., Litvak, V., & Cagnan, H. (2020). State Dependency of Beta Oscillations in the Cortico-Basal-Ganglia Circuit and their Neuromodulation under Phase Locked Inputs, (March), 1–42.

Zavala, B., Damera, S., Dong, J. W., Lungu, C., Brown, P., & Zaghloul, K. A. (2015). Human subthalamic nucleus theta and beta oscillations entrain neuronal firing during sensorimotor conflict. *Cerebral Cortex*, *27*(1), 496–508.

Zavala, B., Jang, A. I., & Zaghloul, K. A. (2017). Human subthalamic nucleus activity during non-motor decision making. *ELife*, *6*, 1–23.

Zavala, B., Jang, A., Trotta, M., Lungu, C. I., Brown, P., & Zaghloul, K. A. (2018). Cognitive control involves theta power within trials and beta power across trials in the prefrontal-subthalamic network. *Brain*, *141*(12), 3361–3376.

Zavala, B., Tan, H., Ashkan, K., Foltynie, T., Limousin, P., Zrinzo, L., … Brown, P. (2016). Human subthalamic nucleus-medial frontal cortex theta phase coherence is involved in conflict and error related cortical monitoring. *NeuroImage*, *137*, 178–187.

Zavala, B., Tan, H., Little, S., Ashkan, K., Hariz, M., Foltynie, T., … Brown, P. (2014). Midline frontal cortex low-frequency activity drives subthalamic nucleus oscillations during conflict. *The Journal of Neuroscience : The Official Journal of*

the Society for Neuroscience, *34*(21), 7322–33.

Zuure, M. B., Hinkley, L. B. N., Tiesinga, P. H. E., Nagarajan, S. S., & Cohen, M. X. (2020). Multiple midfrontal thetas revealed by source separation of simultaneous MEG and EEG. *BioRxiv*, 2020.03.11.987040.

Supplemental Material

Estimating accumulated evidence using computational models

In order to analyse if STN activity reflects the amount of available evidence for each response based on the stimuli presented so far or the Bayesian normalization term (Bogacz & Gurney, 2007), we employed computational models that can estimate these quantities at each point in time. We compared how well different models of evidence accumulation could capture behaviour of different patients, and then generated regressors for each patient based on the best model for that patient.

A basic model in Equation 1 continuously updates the evidence (decision variable, *DV*) for a choice at time *t* based on the existing *DV* from the previous stimuli and the new incoming stimulus S_t, where $S_t = -1$ for the left stimulus, and $S_t = 1$ for the right stimulus. At the start of each trial, the decision variable was initialized to $DV_0 = 0$, and as the decision variable took values further from zero, the probability of making a response increased (see below).

$$DV_t = DV_{t-1} + S_t \quad (1)$$

$$DV_t = (1-\lambda)DV_{t-1} + S_t \quad (2)$$

$$DV_t = DV_{t-1} + \omega_t S_t \quad (3)$$

$$DV_t = (1-\lambda)DV_{t-1} + \omega_t S_t \quad (4)$$

We also considered three extended models which included a forgetting term (λ), a bonus term (ω), or both (Equations 2-4). The forgetting term was used to model the decay of memory over the course of the trial and the bonus term is a weighting of 'same' pairs, i.e. the stimuli which match the directly preceding one (e.g.: in a 'left-left-right' sequence the second left stimulus would be weighted extra as it is the same as the first one).

To estimate the parameters, we assumed that the ratio of making a right choice to making a left choice is related to decision variable according to:

$$\log\frac{P(right)}{P(left)} = \beta_0 + \beta_t DV_t$$

For each participant, we looked for parameters that maximized the likelihood of participant's behaviour after all stimuli shown to that participant.

We found the winning model (based on Bayesian information criterion) to be variable across participants (number of participants in patients/control group indicated): M1 = 1/0; M2 = 0/0; M3 = 4/1; M4 = 8/8, although the model that included both forgetting and bonus terms was the most common. The value of $|DV_t|$ from the best model for a given patient was used as a regressor in Figure 5A.

Strategy Use

In order to analyse the strategy used by the participants, we investigated which factors influence commitment to a choice on a given trial. We considered two factors: The first of them is the evidence integrated for the chosen option according to Equation 1. The second factor we considered was whether the stimulus was the same as the previously presented one, i.e. $SA_t = 1$ if $S_t = S_{t-1}$ and $SA_t = 0$ otherwise. For all stimuli excluding the first stimulus on each trial (for which it is not possible to define SA_t) we performed a logistic regression predicting if the choice has been made after this stimulus, i.e. we tried to predict a variable $D_t = 1$ if choice made after stimulus t and $D_t = 0$ otherwise. For each participant we looked at the significance of the two factors.

There was no participant (among patients and controls) who had a significant second factor ('same' stimulus), but not significant the first factor (evidence). Hence there was no participant who exclusively relied of making a choice after seeing the 'same' stimulus, without considering evidence integrated so far.

	CONTROLS (n)	PATIENTS(n)
Integration	6	6
Combination of integration and pair responses	7	5
Responding to 'same'	0	0
Neither category	0	2

Estimating Bayesian normalization term

In order to create regressors for neural activity recorded from the STN, we used the original proposal that the STN computes the normalization term of the Bayesian equation during the evidence integration process (Bogacz & Gurney, 2007). We defined 2 cortical integrators Y_L and Y_R, which integrate evidence for the left and right stimulus respectively, as described above. Additionally, we subtracted the STN normalization term from the cortical integrators after each stimulus input in a sequence (Bogacz et al., 2016). So, for example, for participants best described by Model 1, the integrators were updated as follows

$$Y_{L,t} = Y_{L,t-1} + L_t - STN_{t-1} \quad (5)$$

$$Y_{R,t} = Y_{R,t-1} + R_t - STN_{t-1} \quad (6)$$

$$STN_t = \log\left(\exp Y_{L,t} + \exp Y_{R,t}\right) \quad (7)$$

In the above equations, $L_t = 1$, $R_t = 0$ if cue t is left, and $L_t = 0$, $R_t = 1$, otherwise. However, for models 2-4 we added decay to the cortical integrators and bonus terms to Equations 5-6 analogously to Equation 2-4. At the start of each trial, the integrators were initialized to $Y_{L,0} = Y_{R,0} = \log 0.5$ (corresponding to equal prior probabilities of the two responses). The value computed from Equation 7 was used as Bayesian normalization regressor in Figure 5.

Table 1: Behavioural Data and Follow-up Statistical Tests. Independent sample t-test revealed significant differences between groups for accuracy and reaction time (ACC: t = -2.99, df = 15.19, p-value = 0.009; RT: t = 2.16, df = 23.37, p-value = 0.041), but not number of stimuli sampled (t = 0.42, df = 23.62, p-value = 0.68). Both groups were similar in their tendency to respond after seeing a 'same' pair (Ratio of responses after 'same': t = -2.01, df = 22.19, p-value = 0.057). The analytical probability of a 'same' pair at the end of the sequence would be 58% if participants chose the moment of response randomly. Both patients and controls responded significantly more often after a 'same' pair (both p<0.001).

PATIENTS	# stimuli seen	ACC	RT	RT 'different'	RT 'same'	ACC 'different'	ACC 'same'	Ratio of responses after 'same' at end
Mean	6.59	0.80	566.07	533.30	608.17	0.65	0.84	0.73
SD	1.88	0.10	57.39	89.17	62.78	0.14	0.10	0.11
SEM	0.52	0.03	15.92	24.73	17.41	0.04	0.03	0.03
Median	6.29	0.84	578.03	572.54	611.90	0.63	0.88	0.78
Min	3.88	0.56	475.62	343.91	508.12	0.47	0.56	0.54
Max	10.12	0.89	650.86	645.10	704.00	0.89	0.94	0.88

CONTROLS	# stimuli seen	ACC	RT	RT 'different'	RT 'same'	ACC 'different'	ACC 'same'	Ratio of responses after 'same' at end
Mean	6.29	0.89	512.85	517.22	522.90	0.77	0.91	0.81
SD	1.65	0.04	67.78	89.75	69.76	0.14	0.03	0.09
SEM	0.46	0.01	18.80	24.89	19.35	0.04	0.01	0.02
Median	5.84	0.90	517.70	528.60	519.55	0.80	0.92	0.79
Min	4.13	0.83	416.90	379.88	416.34	0.42	0.86	0.67
Max	9.11	0.95	636.08	672.74	638.49	0.93	0.96	0.96

Supplementary Figure 1: Effects from Figure 2, plotted for each STN contact separately, rather than averaged over all contacts. We did not find a correlation between contact location and the ‘same’-‘different’ effect. Top: Beta power. Bottom: Theta power.

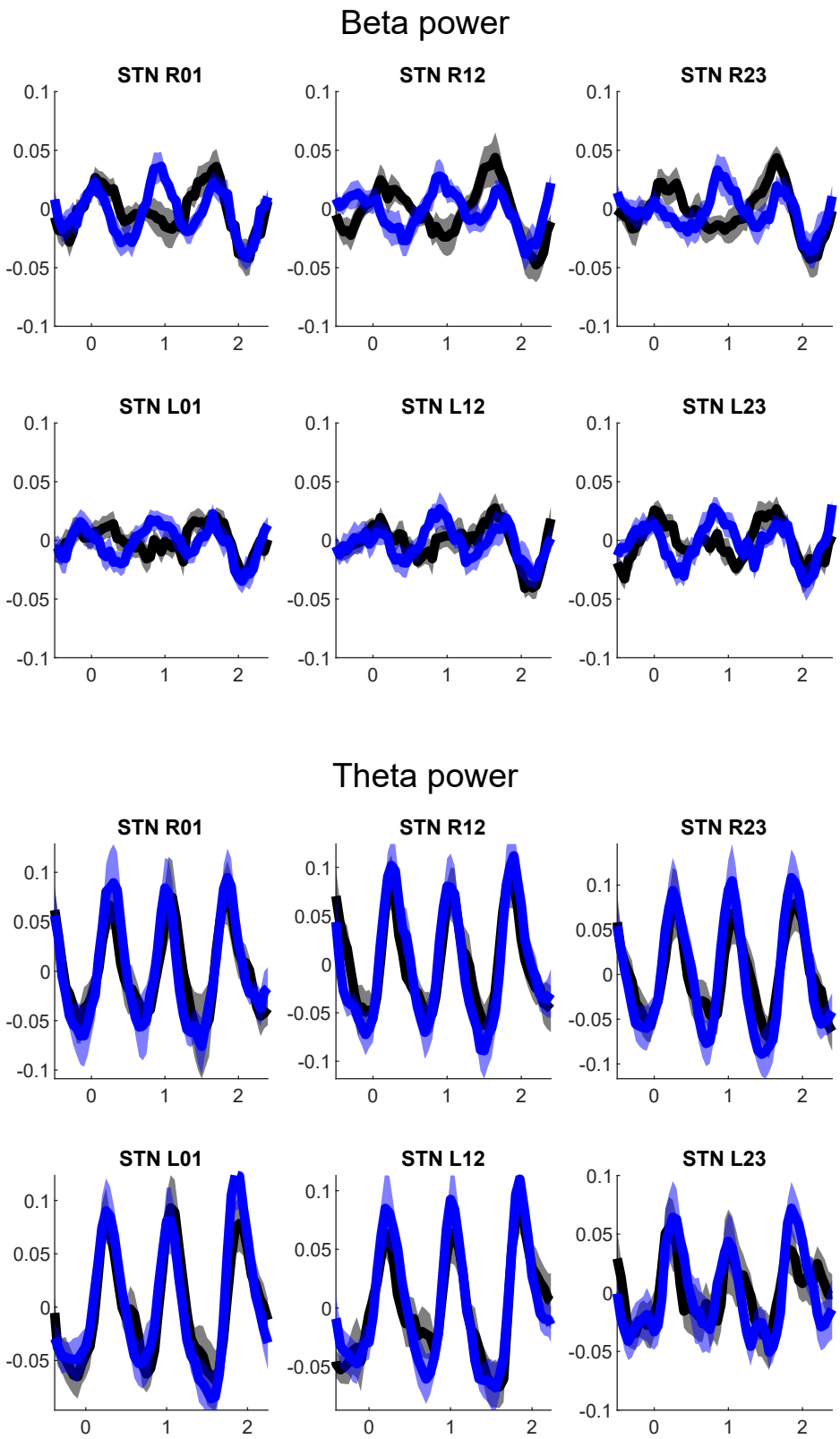
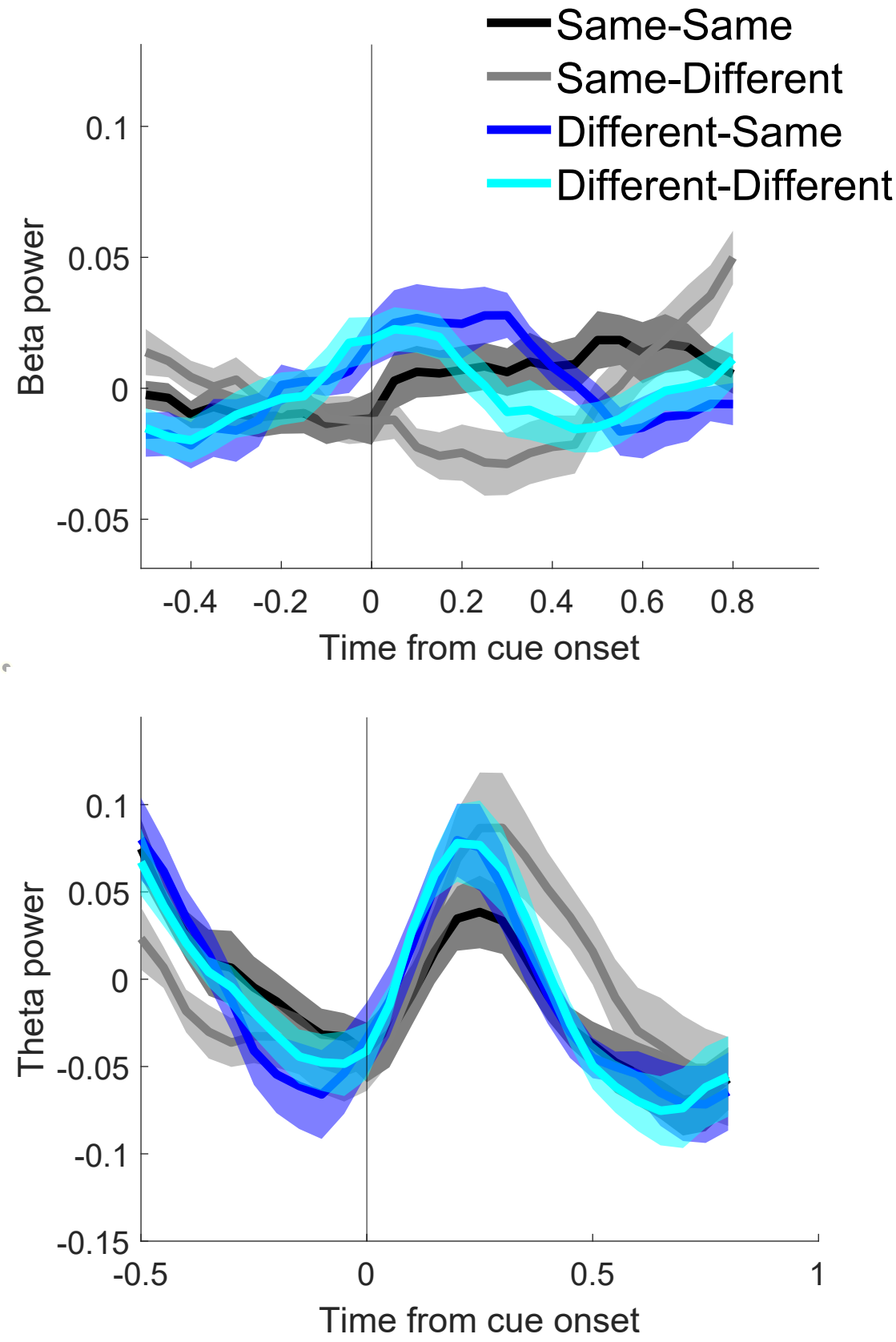
Supplementary Figure 2: Effects from Figure 2, plotted with cue i+1 in detail – for example: ‘same’-‘different’ could be a cue sequence: ‘L-L-R’. Plotted is the response to the last cue of the triplet, ‘R’, in this example. Top: Beta power. Bottom: Theta power.